Plan optimization for mediastinal radiotherapy: Estimation of coronary arteries motion with ECG-gated cardiac imaging and creation of compensatory expansion margins

Plan optimization for mediastinal radiotherapy: Estimation of coronary arteries motion with ECG-gated cardiac imaging and creation of compensatory expansion margins

Mario Levis [a], Viola De Luca [a], Christian Fiandra [a], Simona Veglia [b], Antonella Fava [c], Marco Gatti [d], Mauro Giorgi [c], Sara Bartoncini [a], Federica Cadoni [a], Domenica Garabello [b], Riccardo Ragona [e], Andrea Riccardo Filippi [e,⇑], Umberto Ricardi [a,e]

[a] *Department of Radiation Oncology;* [b] *Department of Radiology;* [c] *Department of Cardiology, AOU Città della Salute e della Scienza, Torino;* [d] *Department of Surgical Sciences; and* [e] *Department of Oncology, University of Torino, Italy*

Radiation therapy (RT) for mediastinal lymphomas and other thoracic tumors frequently entails the involuntary exposure of the whole heart and its substructures. Several studies, conducted on large cohorts of Hodgkin lymphoma and breast cancer long-term survivors, have reported an increased risk of cardiovascular complications and death for those patients who received thoracic RT [1–4]. All these studies indicated a clear relationship between the dose received by the whole heart and the incidence of long-term cardiovascular complications, particularly ischemic events [5,6]. Mean and maximum heart dose have been largely used as dose-volumetric parameters for RT treatment optimization; however, these constraints do not account for the different dose received by important cardiac substructures such as coronary arteries (CA). This dose may be strictly dependent on the definition of the target and organs at risk volume, and modern contouring attitudes include the separate delineation of CA, with the aim of maximally sparing these structures [7]. To date, very few studies [8,9] have explored the correlation between the dose received by CA and long-term events such as coronary stenosis, and CA dose was essentially derived from retrospective studies based on "a posteriori" reconstruction of the treated thoracic volumes. A prospective contouring of CA has not been routinely incorporated into RT treatment flow, mostly due to: (a) the absence of clear dose-constraints; (b) the complexity and time-consuming contouring procedure; (c) the blurring effect, even when adopting intravenous contrast; (d) the difficulty in locating such thin vessels; (e) the uncertainties in quantifying heart-beating related motion. Nevertheless, given that ischemic heart disease is the most relevant cardiac complication after thoracic RT, and that high

dose-gradient techniques such as intensity modulated radiotherapy (IMRT) may allow for a better heart sparing, efforts should be done in better defining CA, also compensating for cardiac motion. In the present study, we aimed to quantify CA motion in relation with cardiac activity, and to estimate an expansion margin that might be able to compensate for CA displacement.

Material and methods

Eight subjects without any cancer history were included in this pilot study. All patients were referred to the Radiological Department of our Hospital between April and May 2016 for a diagnostic ECG-gated CT scan. Our Hospital authorized the retrospective use of the anonymized image set for the study purposes. All ECG-gated CT scans were performed on the same 64 slices CT scanner (Lightspeed VCT Scanner, General Electric Healthcare, Waukesha, WI, USA), with intravenous contrast (Ultravist 370 mg/ml), adopting a dedicated retrospective ECG-gated spiral algorithm [10–12]. A spiral CT scan with continuous table movement and data acquisition was performed; simultaneously, the patient's ECG was recorded and images acquired across different heartbeats, creating a heart phase-consistent sequence. The consequent delineation of CA across all different heart phases allowed for the quantification of coronary motion. All reconstructions were performed in 11% steps over the entire heart cycle, defined as the interval between the R waves (R–R interval) of the QRS complex, leading to the definition of 9 different datasets for each patient, as shown in Fig. 1. All phases were determined as relative to the R peak for every cardiac cycle, and as a percentage of the R–R interval. The end-systole phase was defined as 10–20% and the end-diastole phase as 70–80%, respectively. For images acquisition, patients were asked to hold their breath after a mild hyperventilation. Images were reconstructed at 0.625 mm slice thickness with an increment of 0.4 mm. Those patients with a heart rate >75 beats per minute were medically treated before acquisition. Contrast medium was injected with an 18-gauge catheter at 5 ml per second flow rate. The total contrast dose per patient was roughly 1.0 mg/kg body weight, followed by 50 ml of saline chase at the same flow rate. All 9 (per patient) reconstructed image sets were then exported to Velocity™ (Varian Medical System, Palo Alto, CA, USA) contouring workstation. The following vessels were then contoured on the basis of a "slice by slice" delineation: left main trunk (LM), left anterior descending (LAD), left circumflex (CX) and right coronary artery (RCA), as shown in Fig. 2. All contours were performed by two experienced radiation oncologists according to the atlas published by Feng M et al. [13]. For an optimal visualization, a level of 100 and window of 800 was employed. LM was contoured from its origin to the bifurcation in LAD and CX. The latter trunks were contoured from their origin till the caudal edge of endocardial surface. Septal, diagonal and marginal branches were not contoured. RCA was contoured from its origin to the caudal edge of endocardial surface. Fig. 3 depicts the three-dimensional reconstruction of the coronary tree as contoured for each patient.

With the aim of confirming or not the good contouring quality by radiation oncologists, two cardiac radiologists and two cardiologists were asked to contour the whole coronary tree on one complete image series of 3 patients. They all delineated CA on a "blinded" basis, and contours were then compared for consistency. Two different "references" were adopted for comparison: the most experienced radiologist and the most experienced radiation oncologist. The two cardiologists and the less experienced radiation oncologist and radiologist were considered as comparators for inter-observer evaluation. Contours were assessed by adopting the DICE similarity coefficient, which is a spatial overlap index and a reproducibility validation metric. The DICE similarity coefficient value ranges from 0, indicating no spatial overlap between two volumes, to 1, indicating complete overlap [14]. Center of mass (COM) was estimated for every structure after 3D reconstruction. Displacement of each substructure was then assessed by calculating the difference in COM positioning in all 3 spatial coordinates between the 9 reconstructed images, for each patient. Afterward, an expansion margin (PRV or Planning organ at Risk Volume) was estimated, by applying the McKenzie and van Herk formula [15] for organs at risk (mPRV = 1.3 * R + 0.5 * r), thus accounting both for systematic and random positioning errors. Systematic error is different for each patient and the standard deviation of the combined errors is called R; 1.3 * R ensures that in every single direction the mean position of the distal PRV edge will be

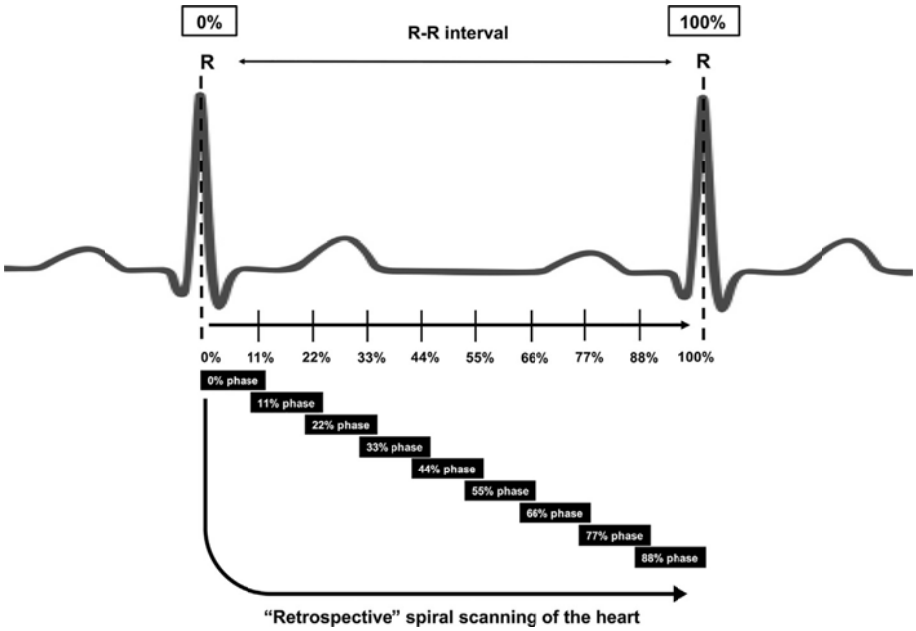

Fig. 1. Outline of the "retrospective algorithm" adopted. Scan data are continuously acquired during the table movements. Image datasets obtained from a complete R–R interval where then reconstructed in 9 cardiac phases.

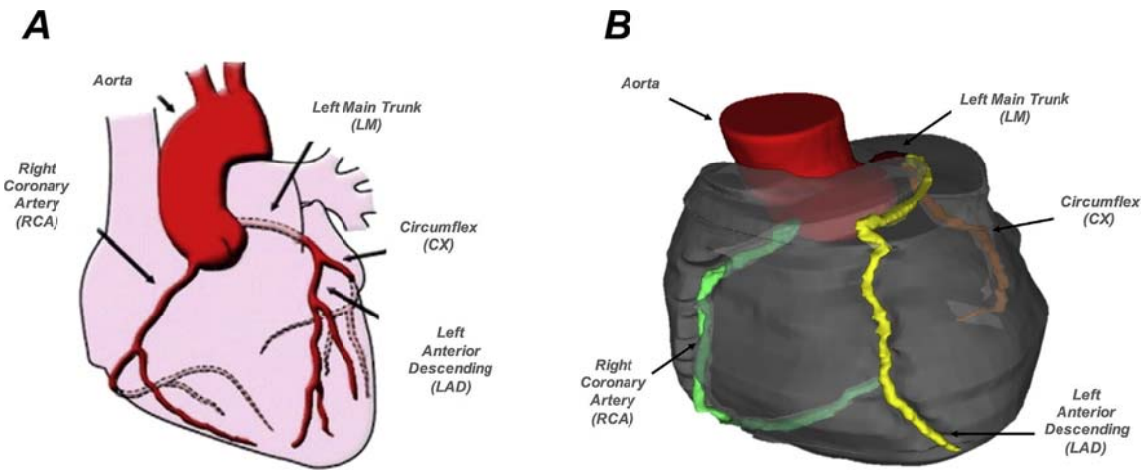

Fig. 2. Coronary anatomy. (A) outline of the coronary arteries. (B) 3D reconstruction of the coronary tree on a mid-diastolic phase (44%) of one patient included in the study.

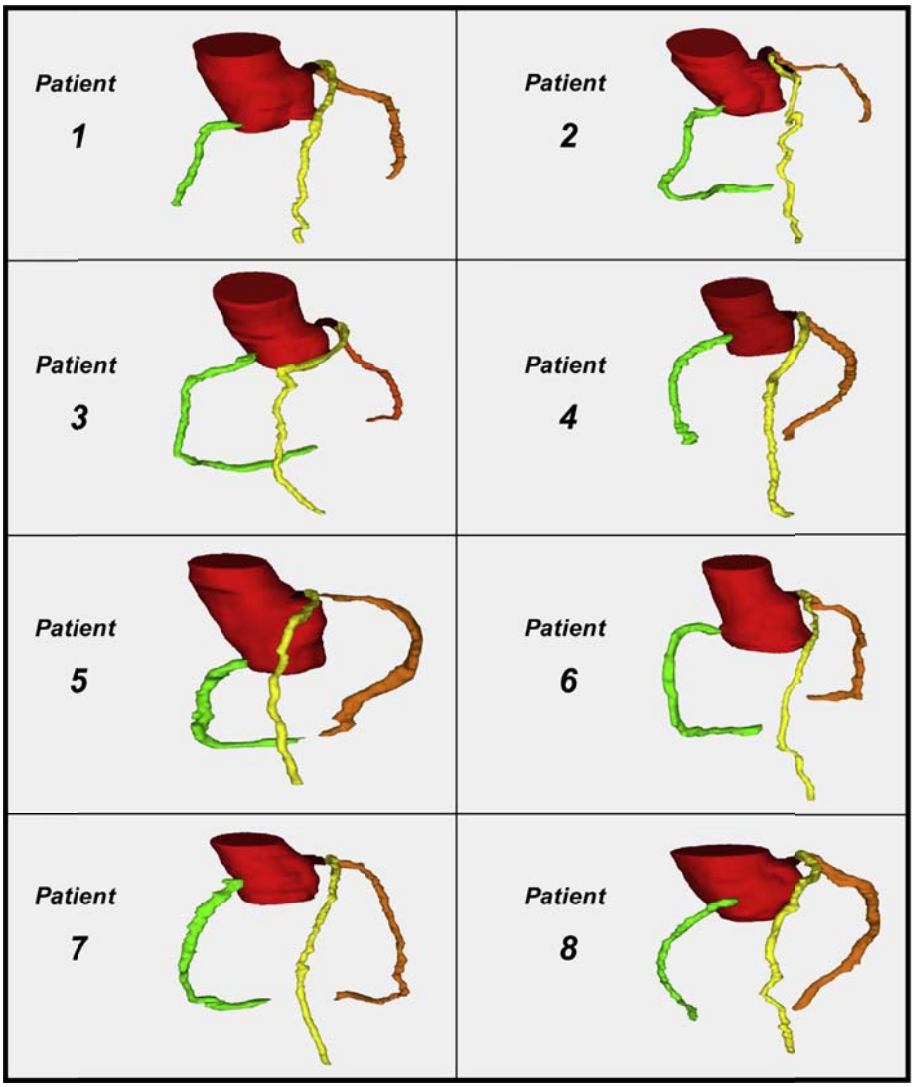

Fig. 3. 3D view (44% phase) of the coronaries contoured for the eight patients enrolled in the study. Colors: Aorta = red; left main trunk = garnet; left descending artery = yellow; circumflex = orange; right coronary artery = green.

encompassed in 90% of plans. Random errors are characterized by standard deviations, which are summed in quadrature to yield a combined value Σ.

Results

Mean age was 63 years old (range 45–75 years). All patients were in sinus rhythm, with an average heartbeat rate of 67 per minute (range 56–89). Mean displacements (mm) of the 4 CA, derived from the 9 samples per 8 patients (for a total of 72 image sets), were calculated according to the McKenzie and van Herk formula in latero-lateral (X), cranio-caudal (Y) and antero-posterior (Z) directions, and are reported in Table 1. Maximum recorded displacement was between 3.6 (for the LM in latero-lateral direction) and 6.9 mm (for the RCA in antero-posterior direction), while mean 3D displacement was 3 mm for LM, 4.8 mm for LAD, 3.9 mm for CX and 5 mm for RCA, respectively. According to these values, we then proposed a specific PRV for CA (Fig. 4), which is reported in Table 1 together with detailed displacements. The inter-observer comparison, estimated on the overall surface of all coronary arteries, showed a good concordance between all clinicians, regardless of the "reference" adopted, with a mean DICE similarity coefficient of 0.64 for experienced radiologist and 0.69 for radiation oncologist (Fig. 5).

Discussion

Thoracic RT may be associated with an increased risk of long-term CA disease, through a multifactorial mechanism involving multiple pathways and converging to inflammatory, cellular, molecular and genetic changes that result in atherosclerotic deposits, thrombosis, endothelial fibrosis and coronary spasms [16,17]. These long-lasting processes, responsible of radiation induced ischemic disease, often require 15–20 years to manifest, but the clinical evolution may be rapid. Particularly, ostial lesions are frequent in patients receiving RT for mediastinal lymphomas [18], because proximal CA segments are frequently the most exposed, being close to the target volumes [9]. This characteristic location of stenotic plaques may be a potentially life-threatening complication, through the abrupt appearance of acute coronary syndrome or sudden death as initial manifestations [19]. The complex cardiac anatomy, made up of muscle, thin arteries and valves, get as result that mean heart dose may not be the better predictor for all types of radiation-related heart diseases. That is particularly true when using high dose-gradient techniques such as IMRT [20–22], when a lower mean heart dose may be achieved, while maintaining an acceptable "low dose bath" on breasts and lungs, but hotspots in critical and small sub-structures such as CA are frequent. Given the well documented correlation between stenosis probability and high-dose hotspots for both breast cancer [8] and Hodgkin lymphoma [9] patients, CA should be regarded as a complex organ at risk that deserves a special attention. A potential strategy is to include CA in the planning optimization process, but several factors hampers this possibility in practice, particularly the difficulties in CA contouring on CT scans and the lack of appropriate constraints to be used for dose optimization. Modern atlases for a correct heart delineation, including CA, have been recently published [13,23], facilitating the contouring process and the incorporation of CA in dosimetric studies. Heart motion represents a serious obstacle for a correct delineation, potentially leading to consistent discrepancies between provisional and truly delivered dose.

In the present study, we focused on CA contouring method, including inter-observer variability, and on the creation of a margin able to compensate for longitudinal, radial and circumferential movements across the whole heart cycle using cardiac gating. Previous studies applied empirical CA margins ranging from 5 mm to 1 cm [24], and inter-observer variability was shown to possibly lead to substantial variation in CA dose estimation (as far as 30%) [25], particularly when these vessels are not contoured by experienced physicians nor in accordance with published guidelines. On the other hand, a recent publication from Wennstig et al. [26] suggested that CA delineation could be reliably reproduced by different radiation oncologists, if well trained, with acceptable inter-observer spatial variation and dose estimation discrepancies.

In our study, we found a good consensus between all observers and the two references, with a DICE index approaching 0.7 for both of them (0.64 for radiologist and 0.69 for radiation oncologist, respectively). With the aim of quantifying the impact of cardiac activity on CA motion and creating an adequate expansion margin, we applied the McKenzie–van Herk formula to CA after an accurate contouring on every phase of the ECG-gated CT scan. In our sample, CA showed different ranges of displacements: first, LAD and RCA had higher ranges of motion than LM and CX; second, we observed that cardiac activity was responsible for heterogeneous movements, with a maximum shift in antero-posterior direction for LAD and RCA, in cranio-caudal direction for CX and latero-lateral direction for LM, respectively. The dissimilar displacements of each CA are justified by asymmetric cardiac motion over the heart cycle and correspond to reported observations [27,28]. Our results are especially consistent with a recent publication from Kataria et al. [29], showing mean systo-diastolic coronary shifts ranging from 4 to 7 mm in breath-hold among a cohort of 20 patients. However, respiratory-induced heart motion was responsible for the larger displacements, particularly in cranio-caudal direction, with a mean range of 7–13 mm in free-breathing. In their study, the Authors extrapolated only 4 reconstructed image sets from the ECG-gated CT scan: end-inspiratory systole, end-inspiratory diastole, end-expiratory systole and end-expiratory diastole. Afterward, they derived the mean shifts by contouring the CA only on these end-systolic and end-diastolic phases, which probably led to an overestimation of the overall cardiac displacements. We adopted a differ-

Table 1
Mean coronary arteries displacements evaluated with the McKenzie–van Herk formula [15] for organs at risk ($mPRV = 1.3 * \Sigma + 0.5 * \sigma$), for the overall population of 8 patients.

Coronary artery	Displacement (mm)			Suggested PRV margin (mm)
	Left-Right (X) Σ and σ	Cranio-caudal (Y) Σ and σ	Antero-posterior (Z) Σ and σ	
Left main trunk (LM)	3.6 0.215 and 0.169	2.7 0.143 and 0.177	2.7 0.143 and 0.162	3
Left anterior descending (LAD)	2.6 0.143 and 0.154	5.0 0.228 and 0.395	6.8 0.413 and 0.291	5
Circumflex (CX)	3.5 0.196 and 0.179	4.5 0.239 and 0.283	3.7 0.183 and 0.256	4
Right (RCA)	3.6 0.169 and 0.276	4.6 0.232 and 0.324	6.9 0.355 and 0.446	5

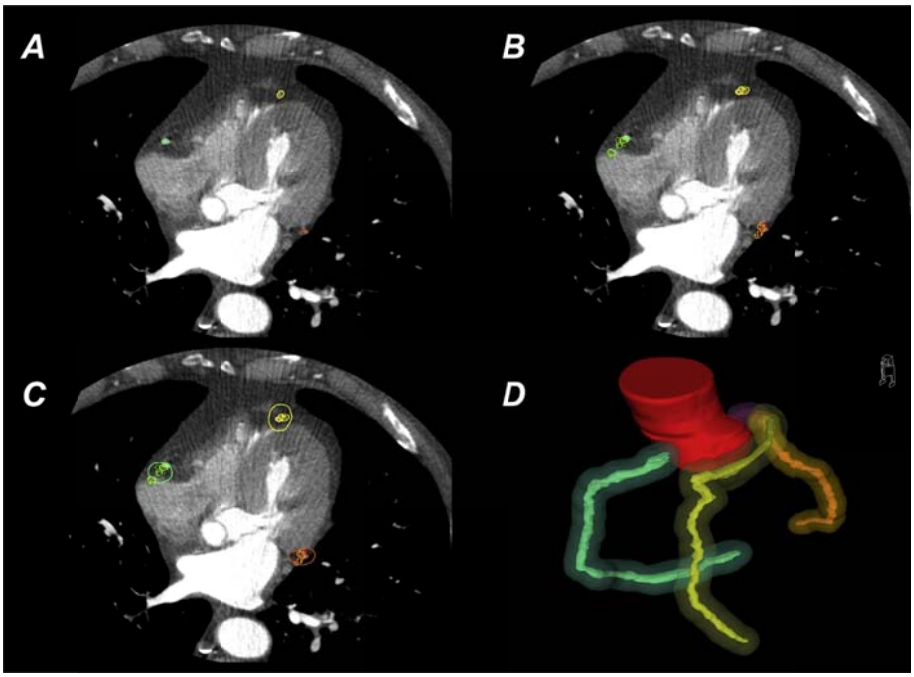

Fig. 4. Model of the expansion margins for the coronary tree. (A) Axial slice (44% phase) showing the contours of circumflex, right and left descending coronaries. (B) Coronary contours, delineated in every cardiac phase, superimposed all together on a mid-diastolic (44%) CT dataset. (C) Axial slice with an example of the coronary expansion margin for circumflex, right and left descending coronaries. (D) 3D reconstruction of the coronaries (solid lines) contoured on the 44% phase with the dedicated PRV (transparent lines). Colors: Aorta = red; left main trunk = garnet; left descending artery = yellow; circumflex = orange; right coronary artery = green.

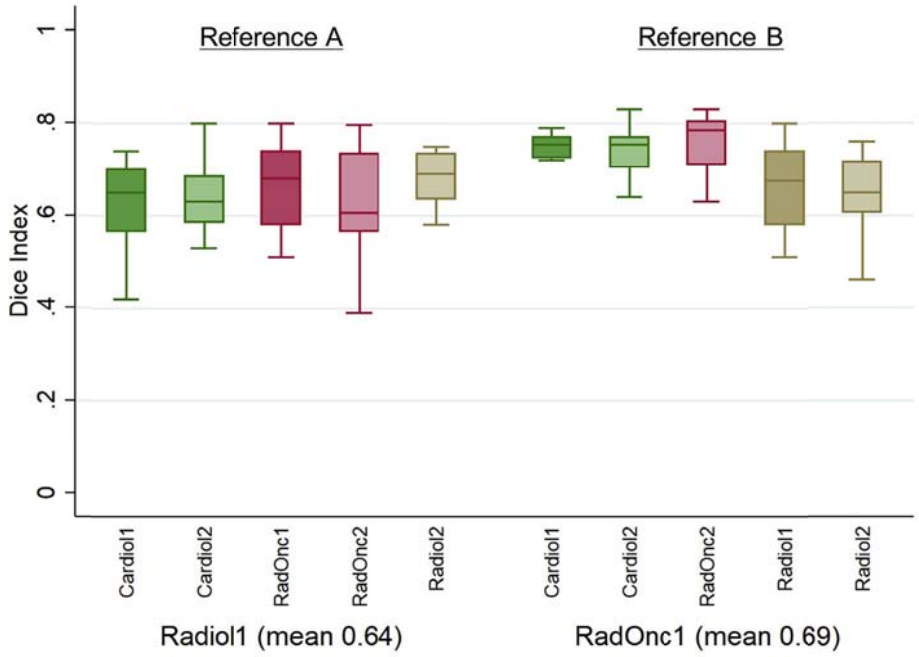

Fig. 5. DICE similarity coefficient between the references and the comparators. Reference A is the most experienced Radiologist, while Reference B is the most experienced Radiation Oncologist. The mean concordance value was 0.64 for Reference A and 0.69 for Reference B.

ent strategy, choosing to contour every single phase that has been segregated by the ECG-gated CT scan. The margins for CA were then estimated by applying a robust methodology, derived by the McKenzie–van Herk formula. Thus, we are confident that in 90% of cases the dose-volume histogram of the PRV would not underestimate the contribution of the high-dose components [15]. The mean displacements along the 3 axes were then combined to obtain a clinically applicable PRV; by this method, we were able to estimate an expansion margin accounting for the different movements (PRV of 3 mm for LM, 4 mm for CX, 5 mm for LAD and RCA, respectively), allowing for a more accurate dose estimation. The major limit of our report is that we did not account for respiratory-related coronary motion, as CT scans were all acquired in breath-holding. Although greater displacements could be

expected in free-breathing, we would like to emphasize that the adoption of respiratory gating is increasingly used in clinical practice, and that the integration of deep inspiration breath holding (DIBH) techniques, together with IMRT, might be of great additional value for heart sparing. Respiratory gating is currently recommended for patients affected with mediastinal lymphomas [30] and breast cancer [31], in reason of the meaningful dosimetric benefit. The expansion margins around CA that we defined, obtained in breath-holding, could be safely adopted to patients receiving thoracic RT, particularly when DIBH is applied. Although this is a preliminary analysis on a limited series, and further investigations would add more precise data on coronary motion, we suggest that our findings might be useful for CA contouring when a radiation course is planned for a heterogeneous group of thoracic malignancies, including left-sided breast cancer.

In conclusion, in the present study CA were shown to be relevantly displaced over the heart cycle when contoured on ECG-gated CT scans, and we suggest to create a PRV by applying an isotropic margin of 3 mm for LM, 4 mm for CX and 5 mm for LAD and RCA, respectively.

Conflict of interest

Nothing to disclose.

Acknowledgments

Nothing to declare.

References

[1] Hancock SL, Tucker MA, Hoppe RT. Factors affecting late mortality from heart disease after treatment of Hodgkin's disease. JAMA 1993;270:1949–55.
[2] Aleman BMP, van den Belt-Dusebout AW, De Bruin ML, et al. Late cardiotoxicity after treatment for Hodgkin lymphoma. Blood 2007;109:1878–86.
[3] Paszat LF, Vallis KA, Benk VMA, Groome PA, Mackillop WJ, Wielgosz A. A population-based case-cohort study of the risk of myocardial infarction following radiation therapy for breast cancer. Radiother Oncol 2007;82:294–300.
[4] Galper SL, Yu JB, Mauch PM, et al. Clinically significant cardiac disease in patients with Hodgkin lymphoma treated with mediastinal radiation. Blood 2011;117:412–8.
[5] Darby SC, Ewertz M, McGale P, et al. Risk of ischemic heart disease in women after radiotherapy for breast cancer. N Engl J Med 2013;368:987–98.
[6] van Nimwegen FA, Schaapveld M, Cutter DJ, et al. Radiation dose-response relationship for risk of coronary heart disease in survivors of Hodgkin lymphoma. J Clin Oncol 2016;34:235–43.
[7] Maraldo MV, Ng AK. Minimizing cardiac risks with contemporary radiation therapy for Hodgkin lymphoma. J Clin Oncol 2016;34:208–10.
[8] Nilsson G, Holmberg L, Garmo H, et al. Distribution of coronary artery stenosis after radiation for breast cancer. J Clin Oncol 2012;30:380–6.
[9] Moignier A, Broggio D, Derreumaux S, et al. Coronary stenosis risk analysis following Hodgkin lymphoma radiotherapy: a study based on patient specific artery segments dose calculation. Radiother Oncol 2015;117:467–72.
[10] Flohr TG, De Cecco CN, Schmidt B, Wang R, Schoepf UJ, Meinel FG. Computed tomographic assessment of coronary artery disease. State-of-the-art imaging techniques. Radiol Clin N Am 2015;53:271–85.
[11] Sun Z. Multislice CT angiography in cardiac imaging: prospective ECG-gating or retrospective ECG-gating? Biomed Imaging Interv J 2010;6:e4.
[12] Sun Z, Ng KH. Prospective versus retrospective ECG-gated multislice CT coronary angiography: a systematic review of radiation dose and diagnostic accuracy. Eur J Radiol 2012;81:e94–e100.
[13] Feng M, Moran JM, Koelling T, et al. Development and validation of a heart atlas to study cardiac exposure to radiation following treatment for breast cancer. Int J Radiat Oncol Biol Phys 2011;79:10–8.
[14] Zou KH, Warfield SK, Bharatha A, et al. Statistical validation of image segmentation quality based on a spatial overlap index. Acad Radiol 2004;11:178–89.
[15] McKenzie A, van Herk M, Mijnheer B. Margins for geometric uncertainty around organs at risk in radiotherapy. Radiother Oncol 2002;62:299–307.
[16] Taunk NT, Haffty BG, Kostis JB, Goyal S. Radiation-induced heart disease: pathologic abnormalities and putative mechanisms. Front Oncol 2015;5:39.
[17] Lenneman CG, Sawyer DB. Cardio-Oncology – An update on cardiotoxicity of cancer-related treatment. Circ Res 2016;118:1008–20.
[18] Mulrooney DA, Nunnery SE, Armstrong GT, et al. Coronary artery disease detected by coronary computed tomography angiography in adult survivors of childhood Hodgkin lymphoma. Cancer 2014;120:3536–44.
[19] Zamorano JL, Lancellotti P, Munoz DR, et al. 2016 ESC position paper on cancer treatments and cardiovascular toxicity developed under the auspices of the ESC committee for practice guidelines. Eur Heart J 2016;37:2768–801.
[20] Maraldo MV, Dabaja BS, Filippi AR, et al. Radiation therapy planning for early-stage Hodgkin lymphoma: experience of the International Lymphoma Radiation Oncology Group. Int J Radiat Oncol Biol Phys 2015;92:144–52.
[21] Filippi AR, Ragona R, Piva C, et al. Optimized volumetric modulated arc therapy versus 3D-CRT for early stage mediastinal Hodgkin lymphoma without axillary involvement: a comparison of second cancers and heart disease risk. Int J Radiat Oncol Biol Phys 2015;92:161–8.
[22] Fiandra C, Filippi AR, Catuzzo P, et al. Different IMRT solutions vs. 3D-Conformal radiotherapy in early stage Hodgkin's lymphoma: dosimetric comparison and clinical consideration. Radiat Oncol 2012;7:186.
[23] Duane F, Aznar MC, Bartlett F, et al. A cardiac contouring atlas for radiotherapy. Radiother Oncol 2017;122:416–22.
[24] Taylor CW, Povall JM, McGale P, et al. Cardiac dose from tangential breast cancer radiotherapy in the year 2006. Int J Radiat Oncol Biol Phys 2008;72:501–7.
[25] Lorenzen EL, Taylor CW, Maraldo M, et al. Inter-observer variation in delineation of the heart and left anterior descending coronary artery in radiotherapy for breast cancer: a multi-centre study from Denmark and the UK. Radiother Oncol 2013;108:254–8.
[26] Wennstig AK, Garmo H, Hallstrom P, et al. Inter-observer variation in delineating the coronary arteries as organs at risk. Radiother Oncol 2017;122:72–8.
[27] Tan W, Xu L, Wang X, Qiu D, Han G, Hu D. Estimation of the displacement of cardiac substructures and the motion of the coronary arteries using electrocardiographic gating. OncoTargets Ther 2013;6:1325–32.
[28] Leter EM, Nowak PJ, Nieman K, et al. Definition of a gross target volume for stereotactic radiation therapy of stented coronary arteries. Int J Radiat Oncol Biol Phys 2002;52:560–5.
[29] Kataria T, Bisht SS, Gupta D, et al. Quantification of coronary artery motion and internal risk volume from ECG gated radiotherapy planning scans. Radiother Oncol 2016;121:59–63.
[30] Rechner LA, Maraldo MV, Vogelius IR, et al. Life years lost attributable to late effects after radiotherapy for early stage Hodgkin lymphoma: the impact of proton therapy and/or deep inspiration breath hold. Radiother Oncol 2017;125:41–7.
[31] Hepp R, Ammerpohl M, Morgenstern C, et al. Deep inspiration breath-hold (DIBH) radiotherapy in left-sided breast cancer. Dosimetrical comparison and clinical feasibility in 20 patients. Strahlenther Onkol 2015;191:710–6.